FEBS Letters 545 (2003) 52–60

FEBS 27215

Minireview

The role of electrostatics in proton-conducting membrane protein complexes

C. Roy D. Lancaster*

Max Planck Institute of Biophysics, Department of Molecular Membrane Biology, Marie-Curie-Str. 15, D-60439 Frankfurt am Main, Germany

Received 4 February 2003; accepted 5 February 2003

First published online 22 April 2003

Edited by Bernard L. Trumpower

Abstract Electrostatic interactions play a key role in the coupling of electron and proton transfer in membrane protein complexes during the conversion of the energy stored in sunlight or reduced substrates into biochemical energy via a transmembrane electrochemical proton potential. Principles of charge stabilization within membrane proteins are reviewed and discussed for photosynthetic reaction centers, cytochrome *c* oxidases, and diheme-containing quinol:fumarate reductases. The impact of X-ray structure-based electrostatic calculations on the functional interpretation of these structural coordinates, on providing new explanations for experimental observations, and for the design of more focused additional experiments is illustrated by a number of key examples.

Key words: Cytochrome *c* oxidase; Electron transfer; Photosynthetic reaction center; Proton transfer; Quinol:fumarate reductase

1. Introduction

Electrostatic interactions play a central role in a variety of biological processes, such as molecular recognition, substrate diffusion, catalytic rates, control by phosphorylation and protein folding (reviewed, e.g., in [1–3]). In particular, they influence biochemical properties such as pK_a values of amino acid side chains and other protonatable groups [4] and redox midpoint potentials of prosthetic groups and cofactors [5]. In the field of bioenergetics, their most important role is the coupling of electron and proton transfer events in respiratory membrane protein complexes. These are essential for the conversion of the energy stored in sunlight or reduced substrates into a transmembrane electrochemical proton potential, which can then, according to the chemiosmotic hypothesis [6], be utilized for the storage of biochemical energy by ATP synthesis.

In order to detail the role of electrostatics in proton-transferring enzymes, this contribution will not only describe some general features of membrane protein electrostatics, but will also illustrate these with two well-investigated examples, the purple bacterial photosynthetic reaction center (RC) and the bacterial cytochrome *c* oxidase (COX). In addition, as an emerging feature, the contribution of electrostatics towards a recently proposed hypothesis of coupled transmembrane electron and proton transfer in diheme-containing quinol:fumarate reductases (QFRs) will briefly be introduced.

This mini-review focuses on the role of ionizable residues in proton-transferring membrane protein complexes, how their charges are stabilized by the protein environment, how they can influence the redox potentials of prosthetic groups and, in turn, how their pK_a values are controlled by the redox state of the cofactors. In this context, the contributions of electrostatic calculations towards mechanistical interpretations of atomic structural coordinates and towards the design of post-structural experiments are discussed.

2. Principles

2.1. Charge-compensating interactions in a membrane protein complex

Fundamentally, there are three ways to stabilize a charge [7]: through reorientation of surrounding dipoles (Fig. 1a), by pre-oriented dipoles in a rigid environment such as the protein interior (Fig. 1b), or through local neutralization by a counter charge (Fig. 1c). In a polar solvent, e.g. for surface-exposed charged groups, stabilization is achieved by rearrangement of solvent dipoles that effectively screen the charge and minimize its long-range effect. Inside a protein, it can be stabilized by pre-oriented dipoles such as the protein backbone or polar side chains. However, in contrast to a polar solvent, such an environment of fixed dipoles is polar but not polarizable. This means that the degree of stabilization of a charge depends upon its position relative to the dipoles and the effect of (de)stabilization is the opposite for positive and negative charges. Examples for how the dipolar environment can stabilize or destabilize charges will be given below. The rigidity of the dipoles and the resulting loss of polarizability is characterized by a low dielectric constant (e.g. $\varepsilon = 4$) inside the

*Fax: (49)-69-6303 1002;
http://www.mpibp-frankfurt.mpg.de/lancaster/index.html.
E-mail address: roy.lancaster@mpibp-frankfurt.mpg.de (C.R.D. Lancaster).

Abbreviations: COX, cytochrome *c* oxidase; H_i^+, a proton from the 'inner' (cytoplasmic or matrix) phase; H_o^+, a proton from the 'outer' (periplasmic or intermembrane) phase; QFR, quinol:fumarate reductase; RC, photosynthetic reaction center; SQORs, succinate:quinone-oxidoreductases; SQR, succinate:quinone reductase; $\Delta G_{crg}(i,j)$, pairwise interaction energy of ionizable residue i with other ionizable residues j; ΔG_{pol}, interaction energy with the protein backbone and polar side chains; ΔG_{rxn}, reaction field energy; μ, dipole length; θ, angle of the dipole axis relative to the position of interest

0014-5793/03/$22.00
doi:10.1016/S0014-5793(03)00393-4

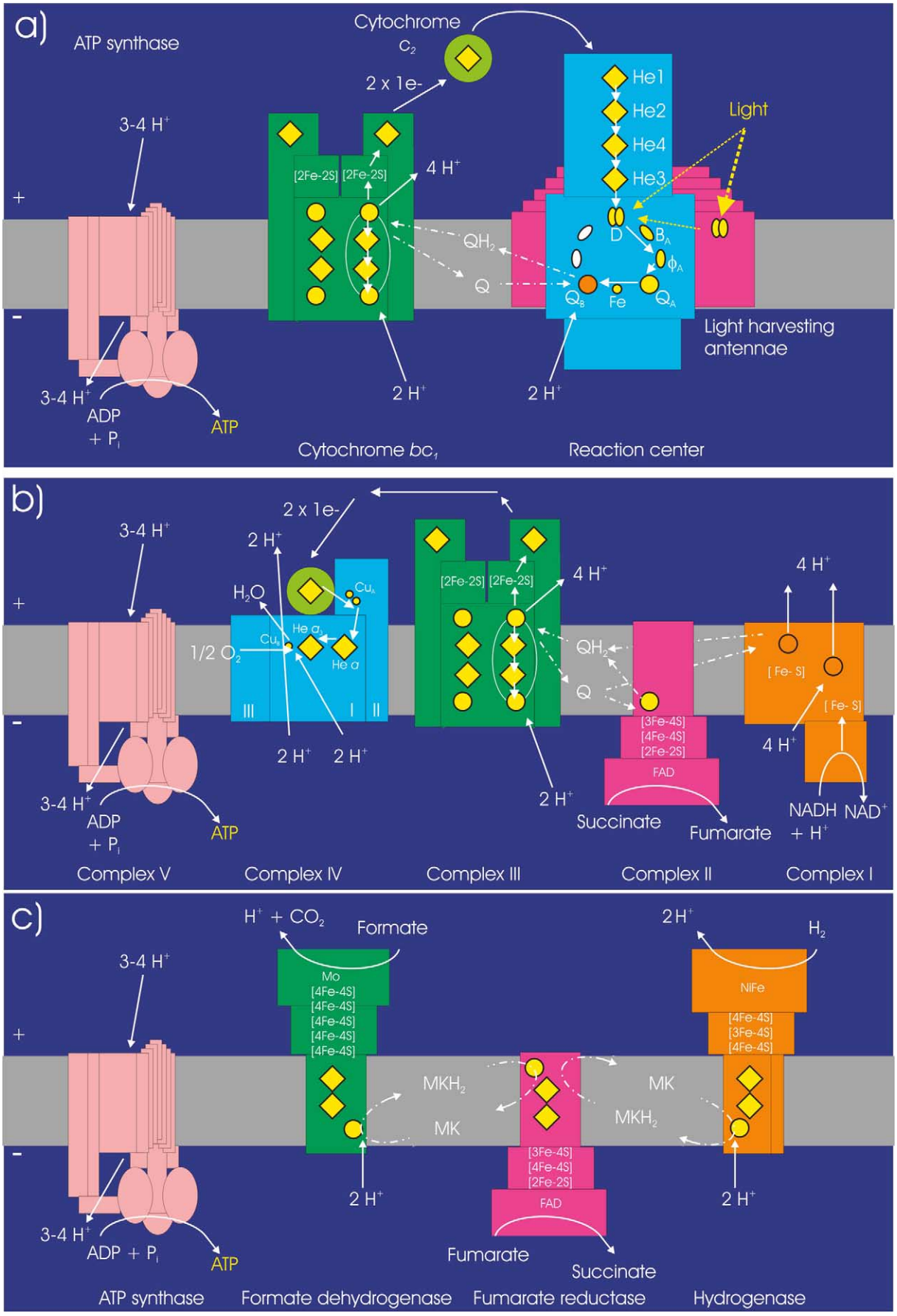
a)
ATP synthase
Cytochrome
c_2
2 x 1e-
3-4 H+
4 H+
[2Fe-2S] [2Fe-2S]
He1
He2
He4
He3
Light
D
B_A
ϕ_A
Q_B
Fe
Q_A
QH_2
Q
Light harvesting
antennae
2 H+
2 H+
3-4 H+
ADP
+ P_i
ATP
Cytochrome bc_1
Reaction center
b)
2 x 1e-
3-4 H+
2 H+
H_2O
Cu_A
Cu_B
He a_3
He a
1/2 O_2
III
I
II
[2Fe-2S] [2Fe-2S]
4 H+
QH_2
Q
[3Fe-4S]
[4Fe-4S]
[2Fe-2S]
FAD
[Fe- S]
[Fe- S]
4 H+
4 H+
2 H+
2 H+
2 H+
3-4 H+
ADP
+ P_i
ATP
Succinate
Fumarate
NADH
+ H+
NAD+
Complex V
Complex IV
Complex III
Complex II
Complex I
c)
$H^+ + CO_2$
Formate
2 H+
H_2
3-4 H+
Mo
[4Fe-4S]
[4Fe-4S]
[4Fe-4S]
[4Fe-4S]
[4Fe-4S]
NiFe
[4Fe-4S]
[3Fe-4S]
[4Fe-4S]
MKH_2
MK
MK
MKH_2
[3Fe-4S]
[4Fe-4S]
[2Fe-2S]
FAD
2 H+
2 H+
3-4 H+
ADP + P_i
ATP
Fumarate
Succinate
ATP synthase
Formate dehydrogenase
Fumarate reductase
Hydrogenase

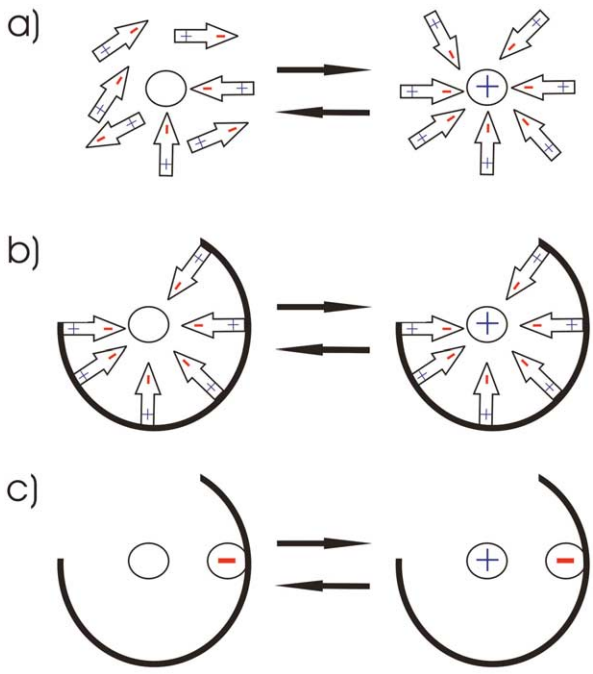

Fig. 1. Three different charge-compensating scenarios (modified from [11]). a: The charge is placed in a medium with a high dielectric constant. b: The charge is stabilized by a set of prearranged dipoles. c: The charge is stabilized by a counter ion.

protein. Thus, buried charges screened by dipoles can have a considerable long-range effect as their potential decreases with $1/\varepsilon r$ while the dipole potential falls of with $\mu \cos \theta/\varepsilon r^2$ (μ is the length of the dipole, θ the angle of the dipole axis relative to the position of interest). In contrast, the third possibility, stabilization by a counter charge of the opposite sign, will diminish the long-range effect of the charge, as the charge pair effectively creates a dipole, the potential of which falls of with $\mu \cos \theta/\varepsilon r^2$.

2.2. *Electrostatic interactions between ionizable residues within the protein*

The role of electrostatic interactions in bioenergetically interesting membrane protein complexes of known three-dimensional structure can be investigated after assigning partial charges and atomic radii to every atom in the coordinate file. Subsequently, electrostatic potentials and interaction energies of potentially charged groups and analysis of the response of the protein environment to redox changes can be calculated by using a continuum dielectric model and finite difference technique [8,9]. The electrostatic free energy of a charged group i in the protein is the sum of at least three different energy terms [10,11]: the reaction field energy (or Born energy [12]) ΔG_{rxn}, which is the result of atoms and electrons in the media stabilizing a charge, the interaction energy ΔG_{pol} with permanent dipoles such as the protein backbone and polar side chains (see below), and the pairwise interaction energies with other ionizable residues j $\Delta G_{\mathrm{crg}}(i,j)$. The latter, in contrast to ΔG_{rxn} and ΔG_{pol}, is dependent on pH and a function of the average protonation of all other ionizable groups j in the protein. Thus, a Monte Carlo sampling method [13,14] is applied to determine the average protonation of all titrating sites in the protein. Groups of residues with strong pairwise electrostatic interactions and thus interdependent ionization states can be referred to as clusters [14]. Given a threshold criterion that these charge–charge interactions change the pK of a residue by two pH units, such clusters have been identified in the examples described below.

3. The purple bacterial photosynthetic RC

In photosynthetic RCs, light-induced electron transfer is coupled to proton uptake from the cytoplasm at the binding site of the so-called 'secondary' quinone, Q_B, where doubly reduced Q_B takes up two protons (Fig. 2a). Although the electrogenic role of the RC alone as a ferrocytochrome c_2:quinone photo-oxidoreductase ([15], Reaction 1, where H_i^+ denotes a proton from the 'inner' or cytoplasmic phase) is based on transmembrane electron transfer and does not involve vectorial proton pumping across the membrane,

$$2\ \mathrm{cyt}\ c_2^{2+} + 2\ \mathrm{H}_i^+ + \mathrm{quinone} \xrightarrow[2\ \mathrm{e}^-]{h\cdot\nu} 2\ \mathrm{cyt}\ c_2^{3+} + \mathrm{quinol} \qquad (1)$$

the interplay of the RC, the cytochrome bc_1 complex and the soluble, periplasmic cytochrome c_2 does lead to the establishment of a transmembrane electrochemical proton potential (Fig. 2a). In addition, the coupling of electron and proton transfer at the Q_B site of the RC may serve as a model for other ubiquinone-reducing or ubiquinol-oxidizing membrane protein complexes (see, e.g., [16,17] for reviews).

←

Fig. 2. Electron and proton transfer in bacterial photosynthesis (a), aerobic (b) and anaerobic (c) respiration. The positive (+) and negative (−) sides of the membrane are indicated. In bacteria, the negative side is the cytoplasm ('inside'), the positive side the periplasm ('outside'). For mitochondrial systems, these are the mitochondrial matrix and the intermembrane space, respectively. Panel a was modified from [15], panels b and c were modified from [44]. a: Photophosphorylation in *R. viridis*. The Q_B site of the RC is highlighted in orange. Light is absorbed by the bacteriochlorophyll of the B1015 light harvesting antennae. Excitation energy is then transferred to a dimer of bacteriochlorophyll, the special pair D, thus forming the excited state D*. This decays through electron transfer via the monomeric accessory bacteriochlorophyll B_A and the bacteriopheophytin ϕ_A to the 'primary electron acceptor', Q_A (which is a menaquinone-9 in the RC of *R. viridis*) leading to the formation of $D^+Q_A^-Q_B$, followed by re-reduction of D^+ by heme 3. These processes can be summarized as a photo-chemical cytochrome oxidation, giving rise to the radical state $DQ_A^-Q_B$. The second step involves the transfer of this first electron to Q_B, a ubiquinone-9 in the *R. viridis* RC, resulting in the state $DQ_AQ_B^-$. After a second photo-chemical cytochrome oxidation in the third step, the diradical state $DQ_A^-Q_B^-$ is formed. While Q_A can only accept one electron, Q_B functions as a 'two-electron gate' [51], and after transfer of a second electron and the first proton, the intermediate state $DQ_A(Q_BH)^-$ is formed in the fourth step. The transfer of the second proton is kinetically indistinguishable from the first proton transfer in the wild-type RC and can only be resolved in the case of mutants with significantly retarded second proton transfer rates [52]. The ubiquinol (Q_BH_2) then leaves its binding site and is re-oxidized by a second membrane protein complex, the cytochrome bc_1 complex, which results in the release of protons on the periplasmic side of the membrane. This proton transport produces a transmembrane electrochemical gradient that drives ATP synthesis through the ATP synthase. The electrons which are released upon quinol re-oxidation are cycled back to the RC via a small soluble protein, cytochrome c_2, and ultimately re-reduce the photo-oxidized tetraheme C subunit. b: Electron flow and the generation and utilization of a transmembrane electrochemical proton potential in aerobic respiration. c: Electron flow and the generation and utilization of a transmembrane electrochemical potential in anaerobic respiration. Menaquinone is abbreviated as MK.

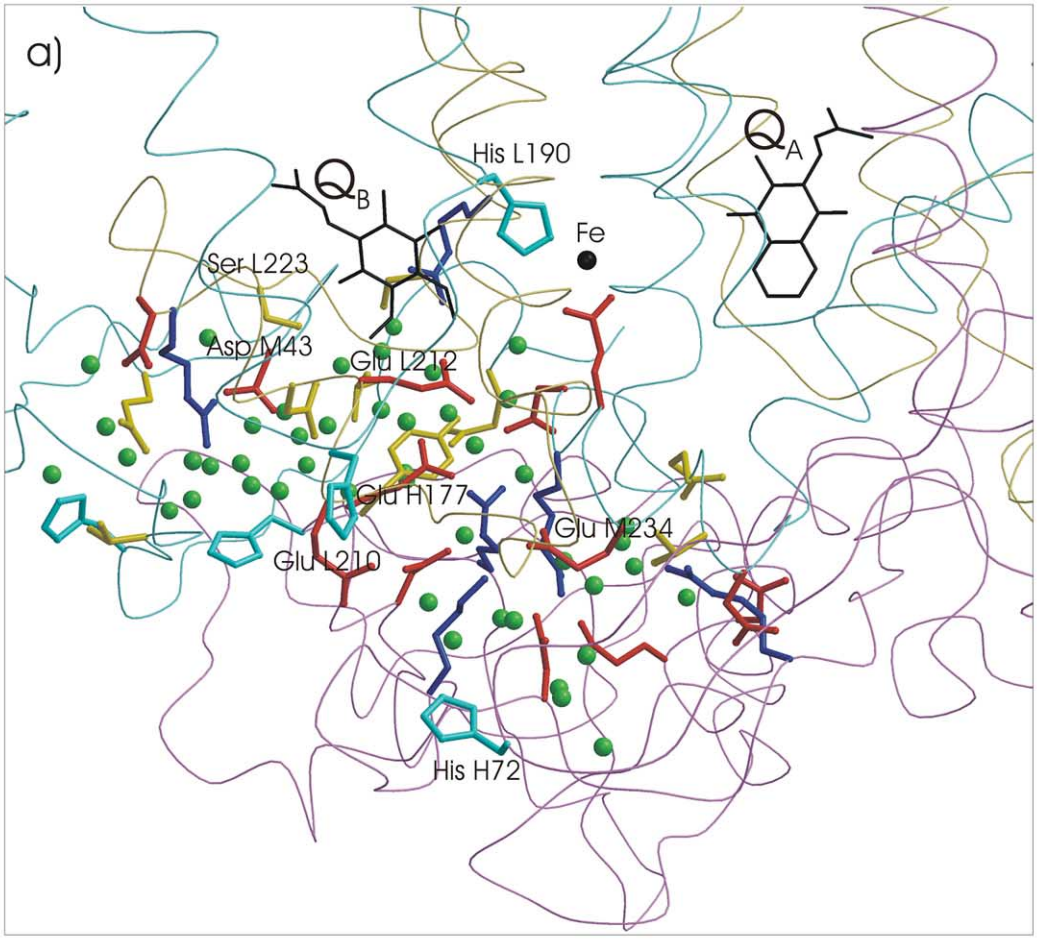

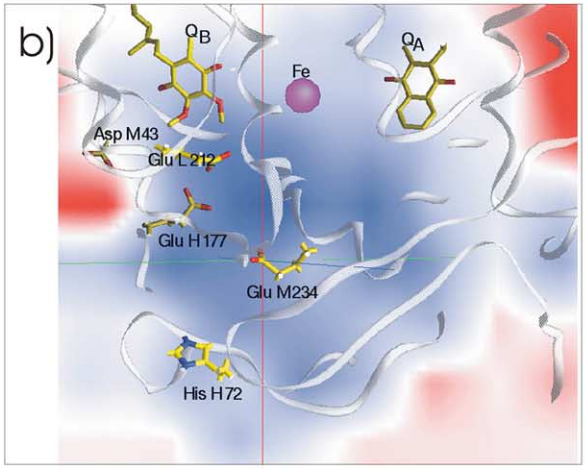

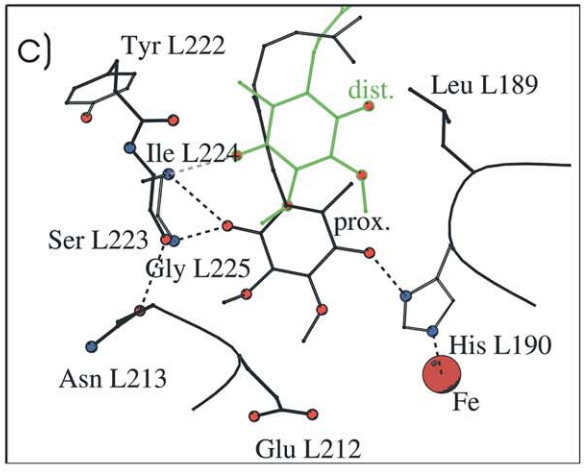

Fig. 3. The *R. viridis* RC. a: Localization of the Q_B cluster within the *R. viridis* RC, as determined in [14]. The coordinate set used is PDB entry 1DXR [53], the Q_B model is from entry 2PRC [21]. The Cα traces of the L, M, and H subunits are drawn in dark yellow, light blue, and pink, respectively. In addition to the members of the cluster, polar side chains and water molecules possibly involved in proton transfer between the cytoplasmic surface and the Q_B site are also shown. Only selected residues are labeled. Side chains of the basic residues Lys and Arg are drawn in blue, those of the acidic residues Asp and Glu in red, His residues in light blue, the polar side chains of Ser, Thr, Tyr, Asn, and Gln in yellow, and water molecules in green. b: Contribution of the polypeptide backbone to the electrostatic potential (from [14]). Depicted is a slice panel parallel to the quinones and the non-heme iron running through the Cδ atom of Glu M234. Positive potential contributions are depicted in blue, negative in red. The respective values for the depicted residues are +460 mV for Glu M234 Cδ, +435 mV for Glu H177 Cδ, +385 mV for Glu L212 Cδ and 0 mV for Asp M43 Cγ. This illustration and Fig. 4b were made with GRASP [54]. c: Comparison of the distal (green, $1PRC_{new}$) and proximal (black, 2PRC) ubiquinone binding sites [21].

The effect of changes in the redox states of both the primary quinone Q_A and the secondary quinone Q_B has been studied by electrostatic calculations on the RCs of *Rhodobacter sphaeroides* [18,19] and *Rhodopseudomonas viridis* [14,20]. In the case of the *R. viridis* RC, an extensive characterization of electrostatically interacting clusters of titrating residues was performed [14]. A cluster of 47 residues was identified, which could be subdivided into a group of 23 residues more strongly coupled to Q_B (the Q_B cluster) and another 24 which are more strongly coupled to Q_A (the Q_A cluster). The Q_B cluster (Fig. 3a) extends for over 33 Å from residue His H72 to the N-terminus of the M subunit, providing several possible entry points for cytoplasmic protons. The Q_B cluster differs from the Q_A cluster in that it has a surplus of acidic residues, a larger number of strong electrostatic interactions, is more buried inside the protein, and experiences a strong positive electrostatic field contribution arising from the polypeptide backbone (Fig. 3b). This dipole field stabilizes the central Q_B cluster residues Glu H177 and Glu M234 (which together with Glu L212 form 'the Glu cluster') in a partially deprotonated form. Consequently, upon reduction of Q_A and Q_B, it is the Glu cluster which is calculated to be responsible for substoichiometric proton uptake by the RC at neutral pH. Due to differences in primary structure, the *R. sphaeroides* RC forms an analogous but different acidic cluster, consisting of Asp L210, Glu L212, and Asp L213 [14,18].

This proton uptake by the Glu cluster also influences the positioning of the quinone substrate Q_B, where two binding sites in the *R. viridis* RC were identified by X-ray crystallography [21]. One of them is the 'proximal' binding site close to the non-heme iron shown in Fig. 3a,b, the other is a 'distal' site, displaced by 4.2 Å along the path of the isoprenoid tail with the quinone ring plane flipped by approximately 180° (see Fig. 3c). Similar results were obtained for the *R. sphaeroides* RC [22,23]. The theoretical electron transfer rate from Q_A^- to Q_B, if calculated as described by Page and colleagues [24], is by 2.5 orders of magnitude (i.e. a factor of 300) faster if Q_B is proximal rather than distal [25]. Molecular dynamics simulations indicate that the preference towards the proximal Q_B location is not necessarily attributable to the reduction of Q_B to the semiquinone, but already to the reduction of the primary quinone Q_A and the resulting protonation changes in the protein [25]. These calculations also suggest a plausible explanation for the observation of predominantly proximally bound Q_B in a Q_A cofactor exclusion variant of the *R. sphaeroides* RC [26], where part of the Q_A site is occupied by a chloride ion. This chloride ion is seen to electrostatically mimic Q_A^-, thus leading to predominantly proximal binding of Q_B [25].

In addition to substoichiometric proton uptake, the negative charge on Q_B^- is calculated to be stabilized by the reorientation of dipoles, especially those of rotatable Ser, Thr, and Tyr hydroxyl groups and of internal water molecules [19]. The most prominent of these changes, that of Ser L223 in the immediate vicinity of the proximal Q_B site, had previously been inferred on the basis of the structures of RC complexes modified at the Q_B site [21].

4. Bacterial COX

In the case of COX, the terminal enzyme of the respiratory chain of mitochondria and many aerobic bacteria (complex IV, see Fig. 2b), which catalyzes electron transfer from cytochrome *c* to molecular oxygen, thereby reducing the latter to water, the redox reaction is coupled to proton translocation across the membrane as shown in Reaction 2 (see [27,28] for a more detailed discussion):

$$4\ \text{cyt}\ c^{2+} + 8\ \text{H}_\text{i}^+ + \text{O}_2 \xrightarrow{4\,e^-} 4\ \text{cyt}\ c^{3+} + 4\ \text{H}_\text{o}^+ + 2\ \text{H}_2\text{O} \qquad (2)$$

where H_o^+ denotes a proton from the 'outer' phase (periplasm or mitochondrial intermembrane space).

Compared to the photosynthetic RC, a comparatively smaller cluster of 18 strongly electrostatically interacting titratable groups were identified in *Paracoccus denitrificans* COX [29], as shown in Fig. 4a. Similar to the RC and despite being buried within the transmembrane part of the protein, most groups of the cluster are calculated to be fully charged at pH 7.0 in the fully oxidized state of the enzyme. Among the few exceptions are the two strongly coupled groups Asp I399 (numbering according to the *Paracoccus* enzyme; see Table 1 for a comparison of the residue numbering) and one of the heme a_3 propionates, that apparently share a single proton, and the neutral Glu I-278, the acidic function of which has been shown to be crucial for proton pumping [30]. It has been suggested that Glu I-278 might play an important role in conferring proton movement on electron transfer [31,32]. In agreement with the electrostatic calculations, Fourier transform infra-red studies on Glu I-278 variant enzymes suggest that this residue is not involved in reduction-induced proton uptake, but rather undergoes conformational changes on reduction of the enzyme or ligand binding [33,34]. It could thus act as a switch [27], transferring protons either to the binuclear center, i.e. the active site of oxygen reduction, or, alternatively, towards a region surrounding the heme propionates [35] from which they could be expelled into the periplasmic phase.

An example is shown in Fig. 4b of how the dipolar environment stabilizes the positive charge on the Arg I-54 side chain, which is conserved among COXs that contain an A-type heme in the low-spin site. The guanidino group of the arginine is hydrogen-bonded to the formyl group of heme *a*, the backbone carbonyl oxygen of residue I-486 and the γ-hydroxyl group of Ser I-490. The polar side chains of Gln I-463, Ser

Table 1
Sequence number conversion table for amino acid residues in subunits (Su) I and II of the COX from *P. denitrificans* (*P.d.*), *R. sphaeroides* (*R.s.*), bovine heart mitochondria (*B.h.m.*), and of the ubiquinol oxidase from *E. coli* (*E.c.*), as discussed in the text

		Residue number			
		P.d.	*R.s.*	*B.h.m.*	*E.c.*
Proton pathways					
D-pathway					
Su I	Asp	124	132	91	135
Su I	Glu	278	286	242	286
K-pathway					
Su I	Tyr	280	288	244	288
Su I	Thr	351	359	316	359
Su I	Lys	354	362	319	362
Su II	Glu	78	101	62	89
Heme *a* environment					
Su I	Arg	54	52	38	80
Heme a_3 environment					
Su I	Asp	399	407	364	407

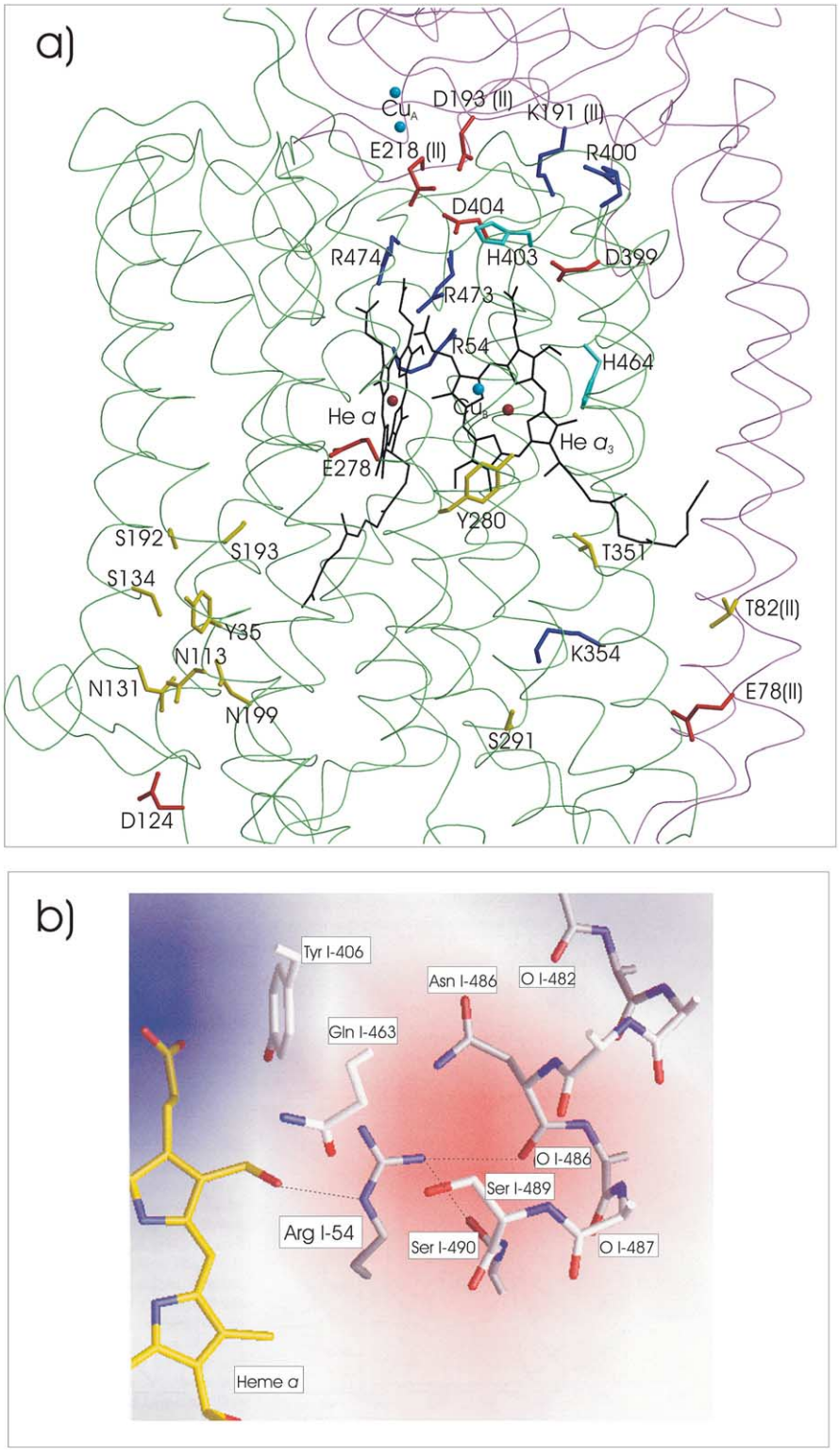

Fig. 4. *P. denitrificans* COX. a: The cluster of strongly interacting ionizable groups as determined in [29] together with the polar residues forming the proposed K- and D-pathways of proton transfer. Color coding of the residue side chains is as described for Fig. 3a. The coordinate set used is PDB entry 1AR1 [55]. b: Contribution of the polypeptide backbone and polar groups to the negative electrostatic potential stabilizing the charge of Arg I-54 (adapted from [36]). Hydrogen bonds are indicated by dotted lines.

I-489, and Ser I-490 and the backbone carbonyl dipoles of residues I-482, I-483, I-486, and I-487 create a region of negative potential stabilizing the positive charge on the arginine. The electrostatic calculations [29] also indicated that the positive charge has a strong influence on the redox potential of the low-spin heme. These results prompted the investigation of the effect of the replacement of Arg I-54 by Met by site-directed mutagenesis [36,37]. The mutation resulted in a blue-

shift of the heme *a* α-band by 15 nm and partial occupation of the low-spin heme site by heme O. Additionally, there was a marked decrease in the midpoint potential of the low-spin heme, resulting in slow reduction of this heme species, and affecting the directionality of electron transfer in the enzyme [36].

Based on the crystal structure of the *Paracoccus* enzyme and in agreement with the results of site-directed mutagenesis studies [38–40], two possible proton transfer pathways were suggested [41]. The shorter one, referred to as the K-pathway, leads to the binuclear center via the highly conserved residues Lys I-354, Thr I-351, and Tyr I-280. The second, longer pathway (D-pathway) involves Asp I-124 and a number of conserved polar residues, then leading to the residue Glu I-278 discussed above. The current view is that these two proton pathways may be associated with different parts of the catalytic cycle. While Asp I-124 was previously identified as a likely proton entry site for the D-pathway, the likely entry site of the K-pathway, Glu II-78, was identified by electrostatic calculations [29] before being confirmed by site-directed mutagenesis studies [42,43].

5. The 'E-pathway hypothesis' of coupled transmembrane electron and proton transfer in diheme-containing QFRs

A first, emerging example of transmembrane proton translocation not associated with the generation of a transmembrane electrochemical potential appears to be the diheme-containing QFR. QFRs and succinate:quinone reductases (SQRs) together form the superfamily of succinate:quinone-oxidoreductases (SQORs) discussed extensively recently [44,45] and also elsewhere in this issue [46]. These enzymes couple the two-electron oxidation of succinate to the two-electron reduction of quinone as well as the reverse reaction (3):

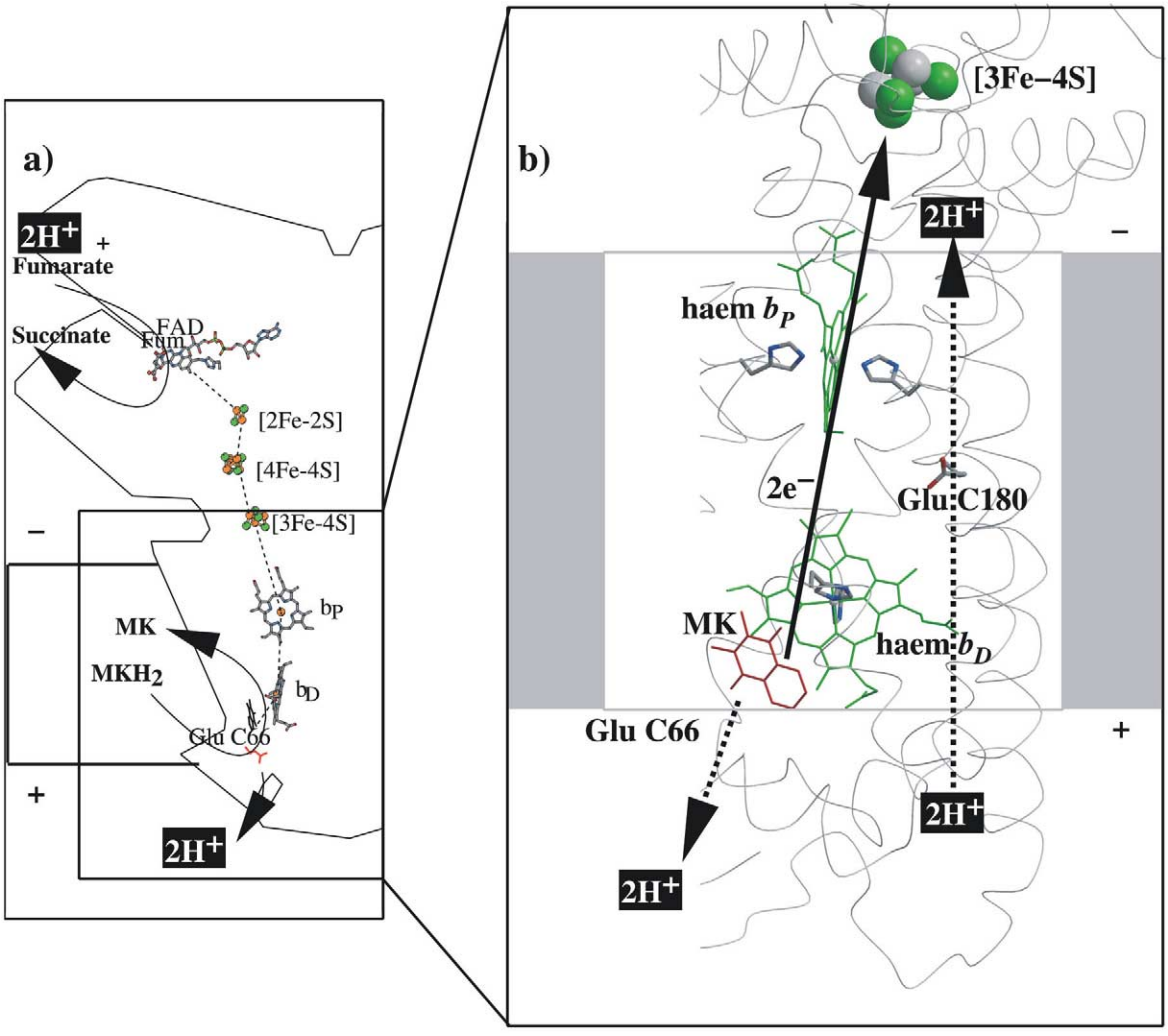

Fig. 5. E-pathway hypothesis of coupled transmembrane proton and electron transfer in *W. succinogenes* QFR. Positive and negative sides of the membrane are described for Fig. 2. a: Hypothetical transmembrane electrochemical potential in the absence of an E-pathway as suggested by the essential role of Glu C66 for menaquinol oxidation by *W. succinogenes* QFR [49]. The prosthetic groups of the *W. succinogenes* QFR dimer are displayed (coordinate set 1QLA; [48]). Distances between prosthetic groups are edge-to-edge distances in Å as defined earlier [24]. Also indicated are the side chain of Glu C66 and a tentative model of menaquinol (MKH_2) binding. The position of bound fumarate (Fum) is taken from PDB entry 1QLB [48]. b: Hypothetical cotransfer of one H^+ per electron across the membrane ('E-pathway hypothesis') [50]. The two protons that are liberated upon oxidation of menaquinol (MKH_2) are released to the periplasm (bottom) via the residue Glu C66. In compensation, coupled to electron transfer via the two heme groups, protons are transferred from the periplasm via the ring C propionate of the distal heme b_D and the residue Glu C180 to the cytoplasm (top), where they replace those protons which are bound during fumarate reduction. In the oxidized state of the enzyme, the 'E-pathway' is blocked.

$$\text{Fumarate} + 2\ H_i^+ + \text{quinol} \overset{2\ e^-}{\rightleftarrows} \text{Succinate} + 2\ H_i^+ + \text{quinone} \quad (3)$$

SQORs generally contain four protein subunits. Among species, the hydrophilic subunits A and B have high sequence homology, while that for the hydrophobic subunits C and D (sometimes replaced by a single large subunit C) is much lower. They also differ in the number of heme *b* groups bound to the hydrophobic domain [47]. For instance *Escherichia coli* QFR contains no heme, while mitochondrial SQR contains one heme *b* group, and both the SQR from the Gram-positive bacterium *Bacillus subtilis* and the QFR from the ε-proteobacterium *Wolinella succinogenes* contain two heme *b* groups. As indicated in Reaction 3, there is little doubt that for the mono-heme and no-heme enzymes the protons bound in the reduction reaction and those released in the oxidation reaction are on the 'inside' (cytoplasm or matrix, respectively). However, the structure of the diheme-containing QFR from *W. succinogenes* indicates that the two hemes are arranged in a manner for efficient transmembrane electron transfer [48] and the site of quinol oxidation has been shown to be oriented towards the periplasm [49], whereas the site of fumarate reduction is oriented towards the cytoplasm. Without compensating events, this arrangement of catalytic sites would indicate that the reaction catalyzed by *W. succinogenes* QFR should be involved in the establishment of a transmembrane proton potential. However, this could not be verified experimentally (see [50] and references therein for a discussion). Instead, it has been proposed [50] that transmembrane electron transfer is strictly coupled to transmembrane proton transfer via a pathway (the so-called 'E-pathway'), involving the residue Glu C180, which is conserved in diheme-containing QFR enzymes (see Fig. 5). This proton transfer thus balances proton release in the periplasm with proton binding in the cytoplasm and consequently makes the whole reaction electroneutral. While this 'E-pathway hypothesis' remains to be proven, it is currently the only working model that adequately explains all experimental findings. Recent electrostatic calculations (A. Haas and C.R.D. Lancaster, manuscript in preparation) indeed indicate that the protonation state of Glu C180 depends on the redox state of the heme groups, which further supports the 'E-pathway hypothesis'.

6. Conclusions

All three principle ways to compensate charges described here are relevant in proton-conducting membrane protein complexes. The balance between these mechanisms is determined by the structure of the respective membrane protein complex. X-ray structure-based electrostatic calculations have been shown to be a valuable tool in the functional interpretation of the structural coordinates, in the development of working hypotheses, in providing explanations for previously unexplained experimental observations, and also in the selection of targets for structure-based mutagenesis experiments.

References

[1] Honig, B. and Nicholls, A. (1995) Science 268, 1144–1149.
[2] Nakamura, H. (1996) Q. Rev. Biophys. 29, 1–90.
[3] Warshel, A. and Papazyan, A. (1998) Curr. Opin. Struct. Biol. 8, 211–217.
[4] Yang, A.S., Gunner, M.R., Sampogna, R., Sharp, K. and Honig, B. (1993) Proteins 15, 252–265.
[5] Gunner, M.R. and Honig, B. (1991) Proc. Natl. Acad. Sci. USA 88, 9151–9155.
[6] Mitchell, P. (1979) Science 206, 1148–1159.
[7] Gunner, M.R., Alexov, E.G., Torres, E. and Lipovaca, S. (1997) J. Biol. Inorg. Chem. 2, 126–134.
[8] Gilson, M.K., Sharp, K.A. and Honig, B. (1987) J. Comp. Chem. 9, 327–335.
[9] Nicholls, A. and Honig, B. (1991) J. Comp. Chem. 12, 435–445.
[10] Gunner, M.R. and Honig, B. (1992) in: The Photosynthetic Bacterial Reaction Center II (Breton, J. and Vermeglio, A., Eds.), pp. 403–410, Plenum Press, New York.
[11] Gunner, M.R. and Alexov, E. (2000) Biochim. Biophys. Acta 1458, 63–87.
[12] Born, M. (1920) Z. Phys. 1, 45–48.
[13] Beroza, P., Fredkin, D.R., Okamura, M.Y. and Feher, G. (1991) Proc. Natl. Acad. Sci. USA 88, 5804–5808.
[14] Lancaster, C.R.D., Michel, H., Honig, B. and Gunner, M.R. (1996) Biophys. J. 70, 2469–2492.
[15] Lancaster, C.R.D. and Michel, H. (2001) in: Handbook of Metalloproteins, Vol. 1 (Messerschmidt, A., Huber, R., Poulos, T. and Wieghardt, K., Eds.), pp. 119–135, Wiley, Chichester.
[16] Lancaster, C.R.D. (1998) Biochim. Biophys. Acta 1365, 143–150.
[17] Lancaster, C.R.D. (1999) Biochem. Soc. Trans. 27, 591–596.
[18] Beroza, P., Fredkin, D.R., Okamura, M.Y. and Feher, G. (1995) Biophys. J. 68, 2233–2250.
[19] Alexov, E.G. and Gunner, M.R. (1999) Biochemistry 38, 8253–8270.
[20] Rabenstein, B., Ullmann, G.M. and Knapp, E.W. (1998) Biochemistry 37, 2488–2495.
[21] Lancaster, C.R.D. and Michel, H. (1997) Structure 5, 1339–1359.
[22] Ermler, U., Fritzsch, G., Buchanan, S.K. and Michel, H. (1994) Structure 2, 925–936.
[23] Stowell, M.H., McPhillips, T.M., Rees, D.C., Soltis, S.M., Abresch, E. and Feher, G. (1997) Science 276, 812–816.
[24] Page, C.C., Moser, C.C., Chen, X. and Dutton, P.L. (1999) Nature 402, 47–52.
[25] Zachariae, U. and Lancaster, C.R.D. (2001) Biochim. Biophys. Acta 1505, 280–290.
[26] McAuley, K.E., Fyfe, P.K., Ridge, J.P., Cogdell, R.J., Isaacs, N.W. and Jones, M.R. (2000) Biochemistry 39, 15032–15043.
[27] Kannt, A. and Michel, H. (2001) in: Handbook of Metalloproteins, Vol. 1 (Messerschmidt, A., Huber, R., Poulos, T. and Wieghardt, K., Eds.), pp. 331–347, Wiley, Chichester.
[28] Mills, D. and Ferguson-Miller, S. (2003) FEBS Lett., this issue.
[29] Kannt, A., Lancaster, C.R.D. and Michel, H. (1998) Biophys. J. 74, 708–721.
[30] Verkhovskaya, M.L., Garcia-Horsman, A., Puustinen, A., Rigaud, J.-L., Morgan, J.E., Verkhovsky, M.I. and Wikström, M. (1997) Proc. Natl. Acad. Sci. USA 94, 10128–10131.
[31] Michel, H. (1998) Proc. Natl. Acad. Sci. USA 95, 12819–12824.
[32] Rich, P.R., Jünemann, S. and Meunier, B. (1998) J. Bioenerg. Biomembr. 25, 165–176.
[33] Hellwig, P., Behr, J., Ostermeier, C., Richter, O.M.H., Pfitzner, U., Odenwald, A., Ludwig, B., Michel, H. and Mäntele, W. (1998) Biochemistry 37, 7390–7399.
[34] Puustinen, A., Bailey, J.A., Dyer, R.B., Mecklenburg, S.L. and Wikström, M. (1997) Biochemistry 36, 13195–13200.
[35] Behr, J., Hellwig, P., Mäntele, W. and Michel, H. (1998) Biochemistry 37, 7400–7406.
[36] Kannt, A., Pfitzner, U., Ruitenberg, M., Hellwig, P., Ludwig, B., Mäntele, W., Fendler, K. and Michel, H. (1999) J. Biol. Chem. 274, 37974–37981.
[37] Riistama, S., Verkhovsky, M.I., Laakonen, L., Wikström, M. and Puustinen, A. (2000) Biochim. Biophys. Acta 1456, 1–4.
[38] Garcia-Horsman, J.A., Puustinen, A., Gennis, R.B. and Wikström, M. (1995) Biochemistry 34, 4428–4433.
[39] Hosler, J.P., Ferguson-Miller, S., Calhoun, M.W., Thomas, J.W., Hill, J., Lemieux, L., Ma, J.X., Georgiou, C., Fetter, J., Shapleigh, J., Tecklenburg, M.M.J., Babcock, G.T. and Gennis, R.B. (1993) J. Bioenerg. Biomembr. 25, 121–136.

[40] Thomas, J.W., Puustinen, A., Alben, J.O., Gennis, R.B. and Wikström, M. (1993) Biochemistry 32, 10923–10928.
[41] Iwata, S., Ostermeier, C., Ludwig, B. and Michel, H. (1995) Nature 376, 660–669.
[42] Ma, J.X., Tsatsos, P.H., Zaslavsky, D., Barquera, B., Thomas, J.W., Katsonouri, A., Puustinen, A., Wikström, M., Brzezinski, P., Alben, J.O. and Gennis, R.B. (1999) Biochemistry 38, 15150–15156.
[43] Bränden, M., Tomson, F., Gennis, R.B. and Brzezinski, P. (2002) Biochemistry 41, 10794–10798.
[44] Lancaster, C.R.D. (2001) in: Handbook of Metalloproteins, Vol. 1 (Messerschmidt, A., Huber, R., Poulos, T. and Wieghardt, K., Eds.), pp. 379–401, Wiley, Chichester.
[45] Lancaster, C.R.D. (2002) Biochim. Biophys. Acta 1553, 1–176.
[46] Cecchini, G., Maklashina, E., Yankovskaya, V., Iverson, T.M. and Iwata, S. (2003) FEBS Lett., this issue.
[47] Hägerhäll, C. and Hederstedt, L. (1996) FEBS Lett. 389, 25–31.
[48] Lancaster, C.R.D., Kröger, A., Auer, M. and Michel, H. (1999) Nature 402, 377–385.
[49] Lancaster, C.R.D., Gross, R., Haas, A., Ritter, M., Mäntele, W., Simon, J. and Kröger, A. (2000) Proc. Natl. Acad. Sci. USA 97, 13051–13056.
[50] Lancaster, C.R.D. (2002) Biochim. Biophys. Acta 1565, 215–231.
[51] Wraight, C.A. (1982) in: Function of Quinones in Energy Conserving Systems (Trumpower, B.L., Ed.), pp. 181–197, Academic Press, New York.
[52] McPherson, P.H., Schonfeld, M., Paddock, M.L., Okamura, M.Y. and Feher, G. (1994) Biochemistry 33, 1181–1193.
[53] Lancaster, C.R.D., Bibikova, M.V., Sabatino, P., Oesterhelt, D. and Michel, H. (2000) J. Biol. Chem. 275, 39364–39368.
[54] Nicholls, A., Sharp, K.A. and Honig, B. (1991) Proteins 11, 281–296.
[55] Ostermeier, C., Harrenga, A., Ermler, U. and Michel, H. (1997) Proc. Natl. Acad. Sci. USA 94, 10547–10553.